Supporting Information (SI)

Exploring the properties of Zr_2CO_2/GaS van der Waals heterostructures for Optoelectronic Applications

Altaf Ur Rahman,[1,2] M. Abdul,[1,*] Altaf Karim,[3] Gul Rahman,[4,†] Islam H. El Azab,[5] and Bao Jingfu[1,‡]

[1]*School of Integrated Circuit Science and Engineering, University of Electronic Science and Technology of China, Sichuan Chengdu, People's Republic of China*

[2]*Department of Physics, Riphah International University, Lahore, Pakistan.*

[3]*Department of Physics, COMSATS University Islamabad, 44000, Pakistan*

[4]*Department of Physics, Quaid-i-Azam University Islamabad, 44000, Pakistan*

[5]*Department of Food Science and Nutrition, College of Science, Taif University, P.O. box 11099, Taif 21944, Saudi Arabia*

(Dated: June 10, 2024)

* mabdul@mail.ustc.edu.cn

† gulrahman@qau.edu.pk

‡ baojingfu@uestc.edu.cn

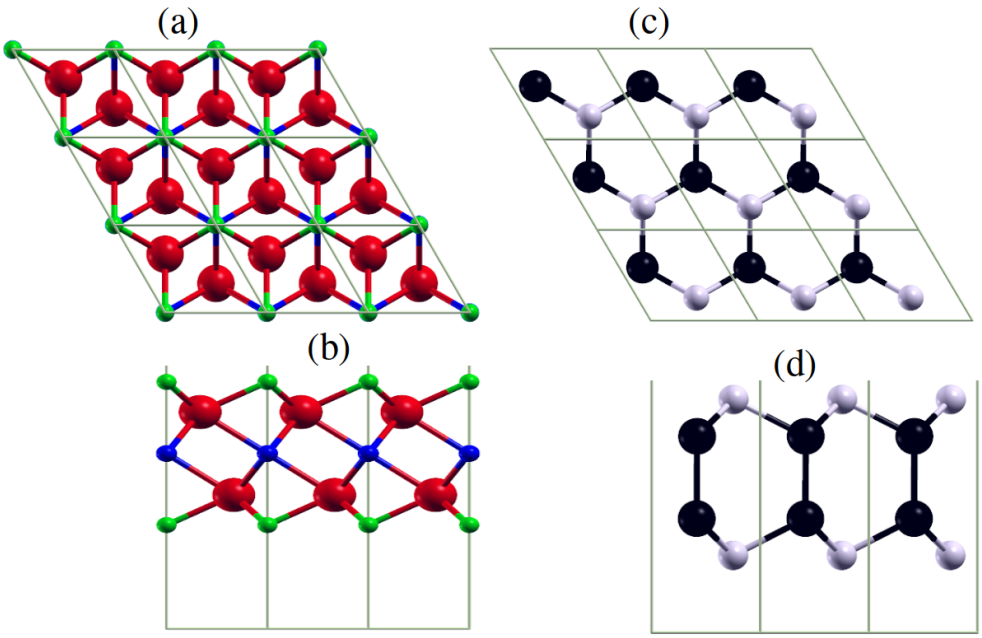

Figure SI 1: Schematic $3 \times 3 \times 1$ supercell representations of top-view (upper panel) and side-view (bottom panel) of a pristine (a, b) Zr_2CO_2 monolayer (MD4 configuration) and (c, d) GaS monolayer. The red, blue, green, black and white colors spheres represents Zr, C, O, Ga and S atoms, respectively.

I. COMPUTATIONAL METHODS AND MODELING

All the calculations were carried out in the framework of Density functional theory (DFT) [1] as implemented in the Quantum Espresso (QE) package [2]. The plane-wave and ultra-soft pseudo-potentials were used to perform the calculations. We used the generalized gradient approximation (GGA) calculating the exchange correlation interactions proposed by Perdew, Burke, and Ernzerhof (PBE) [3]. The electron wave functions were expressed in term of a plane wave basis set with kinetic energy and charge density cutoffs of value 60 Ry and 300 Ry, respectively.

The Monkhorst-Pack method [4] was used for creating k-meshes in the first Brillouin-zone (BZ). A $12 \times 12 \times 1$ k-mesh was employed for geometric optimization, whereas a dense $20 \times 20 \times 1$ k-mesh was employed to calculate the total density of states (TDOS) and the optical characteristics of both isolated monolayers and vdW heterostructures. The van vdW interaction between the slabs was treated using the Grimme DFT-D2 correction. It is necessary to employ a vacuum thickness greater than 15 Å to prevent the interactions between the adjacent slabs. We thoroughly examined the convergence of results for each and every computational parameter. For crystal

structure optimization, all the atomic position of atoms were permit to relax until the Hellmann-Feynman forces were get smaller than 0.003 Ry/Bohr. We estimated the formation energy to ensure structural integrity, which is defined as

$$E_f = \{E_{\text{tot}[Zr_2CO_2]} - 2E_{\text{tot}[Zr]} - 2E_{\text{tot}[O]} - E_{\text{tot}[C]}\}) \quad (1)$$

where $E_{\text{tot}[Zr_2CO_2]}$ represent the ground state energy of Zr_2CO_2 monolayer and $E_{\text{tot}[Zr]}$, $E_{\text{tot}[C]}$, and $E_{\text{tot}[O]}$ represents the ground state energy per zirconium atom, carbon atom and oxygen atoms in its lowest chemical-potential phase, respectively. The lowest chemical-potential of the Zr/C atom is calculated using its natural occurring phase (HCP: Hexagonal Closed Packed), which consists of two constituent atoms in its primitive unit cell. The total energy of the oxygen molecule (O_2), which consists of two atoms of oxygen is utilized to determine the total energy of atomic oxygen. The accuracy of electronic characteristics is essential for determining the catalytic mechanism of GaS and Zr_2CO_2 monolayers as well as the Zr_2CO_2/GaS van der Waal heterostructures. It is well known that the GGA+PBE energy functional typically underestimates the semiconductor band gap [5]. Therefore, in order to precisely calculate the electrical and optical characteristics of 2D GaS, Zr_2CO_2, and Zr_2CO_2/GaS van der Waal heterostructure, we used Heyd–Scuseria–Ernzerhof (HSE) functional [6]. We employed the hybrid functional to solve the band gap problem by combining the Hartree-Fock and DFT exchange terms [7]. The mixing parameter governing how much Hartree-Fock exchange is incorporated in the hybrid functional is called the "fraction of exchange" (α). To increase the precision of electronic structure calculations, the semi-local and non-local screened Hartree-Fock exchange combined in the HSE hybrid functional. If = 0.20, then 80 % of semi-local and 20 % of Hartree-Fock exchanges are combined. For HSE calculations, the fraction of exchange (α) of amount 0.20 and exchange screening parameter (β) set to 0.12 are used which can reproduce the experimental bandgap of GaS, Zr_2CO_2 monolayers and Zr_2CO_2/GaS van der Waal heterostructures.

Optical properties of materials are important for potential use in optical devices and electronic detectors. When electromagnetic radiation passes through a material then various phenomena take place due to the interaction light-matter such as reflection, transmission, and absorption. Optical characteristics of a materials are investigated in terms of these parameters [8, 9]. Among which, one of the important and basic parameters is the complex part of the dielectric function $\epsilon(\omega)$. The complex part $\epsilon_2(\omega)$ is directly related to the material linear response to solar light irradiation. The dielectric function $\epsilon(\omega)$ is expressed in terms of real $\epsilon_1(\omega)$ and complex parts $\epsilon_2(\omega)$ mathematically as;

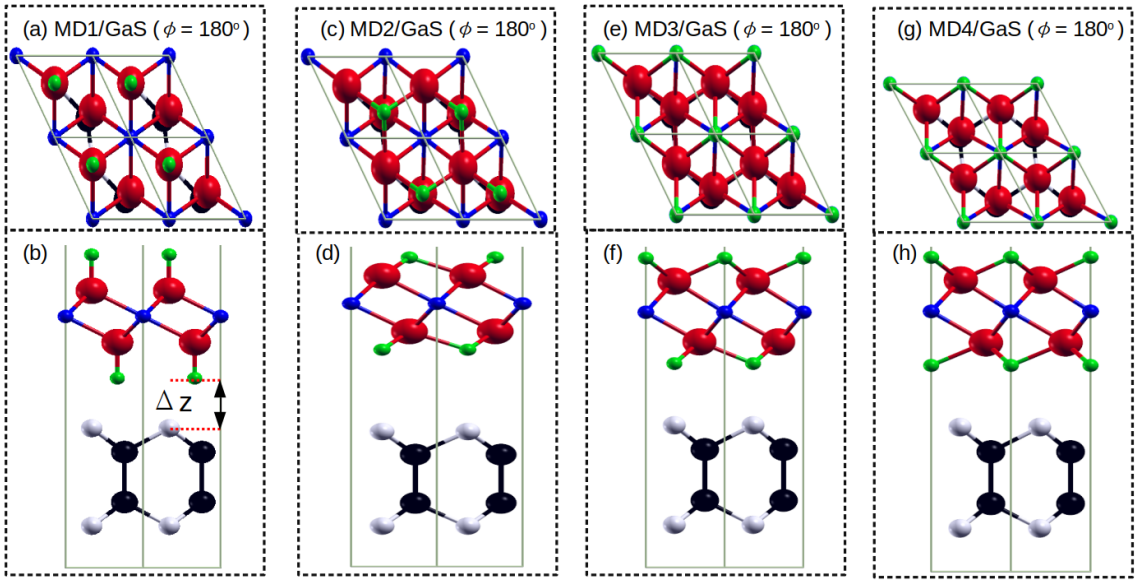

Figure SI 2: (a, b) MD1/GaS ($\phi = 180^o$), (c, d) MD2/GaS ($\phi = 180^o$) (e, f) MD3/GaS ($\phi = 180^o$) (g, h) MD4/GaS ($\phi = 180^o$). Zr, C, O, Ga and S atoms are represented by red, blue, green, black and white colors spheres, respectively.

$$\epsilon(\omega) = \epsilon_1(\omega) + \iota\epsilon_2(\omega) \tag{2}$$

The imaginary part $\epsilon_2(\omega)$ contain the information about how much total energy of the incident photon is absorbed by system. The complex part can be obtained using the basis of RPA (RPA: Random Phase Approximation) [10, 11];

$$\epsilon_2(\omega) = \frac{4\pi^2 e^2}{m^2\omega^2} \sum_{i,j} \int_k \langle i|M|j\rangle^2 f_i(1-f_i) \times \delta(E_{j,k} - E_{i,k} - \omega) d^3k \tag{3}$$

Here, the integrand represents the dipole matrix, i and j represent ground and excited states, the corresponding ground state energy indicated by E_i, excited state energy indicated by E_f and f_i denotes the Fermi-distribution function of the ground level. To connect mathematically the real and imaginary part of the dielectric functions the set of Kramers-Kronig relations are used [12]. This can be mathematically expressed as;

$$\epsilon_1(\omega) = 1 + \frac{2}{\pi} P \int_0^\infty \frac{\omega' \epsilon_2(\omega')}{(\omega'^2 - \omega^2)} d\omega \tag{4}$$

The improper value of the above integral is captured by the Cauchy principle value denoted by P. The other optical parameter can be expressed in term of $\epsilon_1(\omega)$ and $\epsilon_2(\omega)$. To characterize how incident photon interacts with a material, we can define index of refraction which is itself a complex

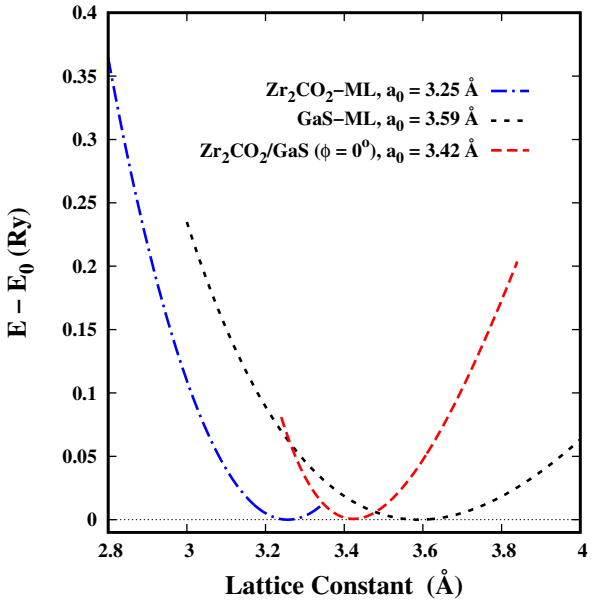

Figure SI 3: GGA+PBE calculated lattice constant optimization of pristine Zr_2CO_2 (MD4 configuration) and GaS monolayers. The blue and black colors represent the lattice constant plot of pristine Zr_2CO_2 (MD4) and GaS monolayers, respectively. Considering the most stable Zr_2CO_2(MD4)/GaS vdW heterostructure $\phi = 0^o$ configuration, we did optimization of the lattice constant. The red dashed line indicates the lattice constant optimization of Zr_2CO_2/GaS vdW hetero structure ($\phi = 0^o$).

quantity consisting of both real and imaginary parts, the real part know is refractive index and imaginary part termed as extinction coefficient [13]. Mathematically it can be expressed as;

$$\bar{n}(\omega) = n(\omega) + \iota k(\omega) \tag{5}$$

The real part of the index of refraction tells us how much the speed of an incident photon slows down as it passes through a material compared to the speed of light. The imaginary part describing attenuation (absorption) of incident photon as it passes through material medium [14]. The refractive index and extinction coefficients can be written in term of $\epsilon_1(\omega)$ and $\epsilon_2(\omega)$, as given below

$$n(\omega) = (1/\sqrt{2}) \left[\sqrt{\epsilon_1^2(\omega) + \epsilon_2^2(\omega)} + \epsilon_1(\omega) \right]^{1/2} \tag{6}$$

and

$$k(\omega) = (1/\sqrt{2}) \left[\sqrt{\epsilon_1^2(\omega) + \epsilon_2^2(\omega)} - \epsilon_1(\omega) \right]^{1/2} \tag{7}$$

Similarly, to measure how much incident photon energy is reflected back from a material surface rather than being absorbed, we can define reflection coefficient R(ω) [15], The R(ω) can be derived from in real and imaginary part of the index of refraction. R(ω) as given below:

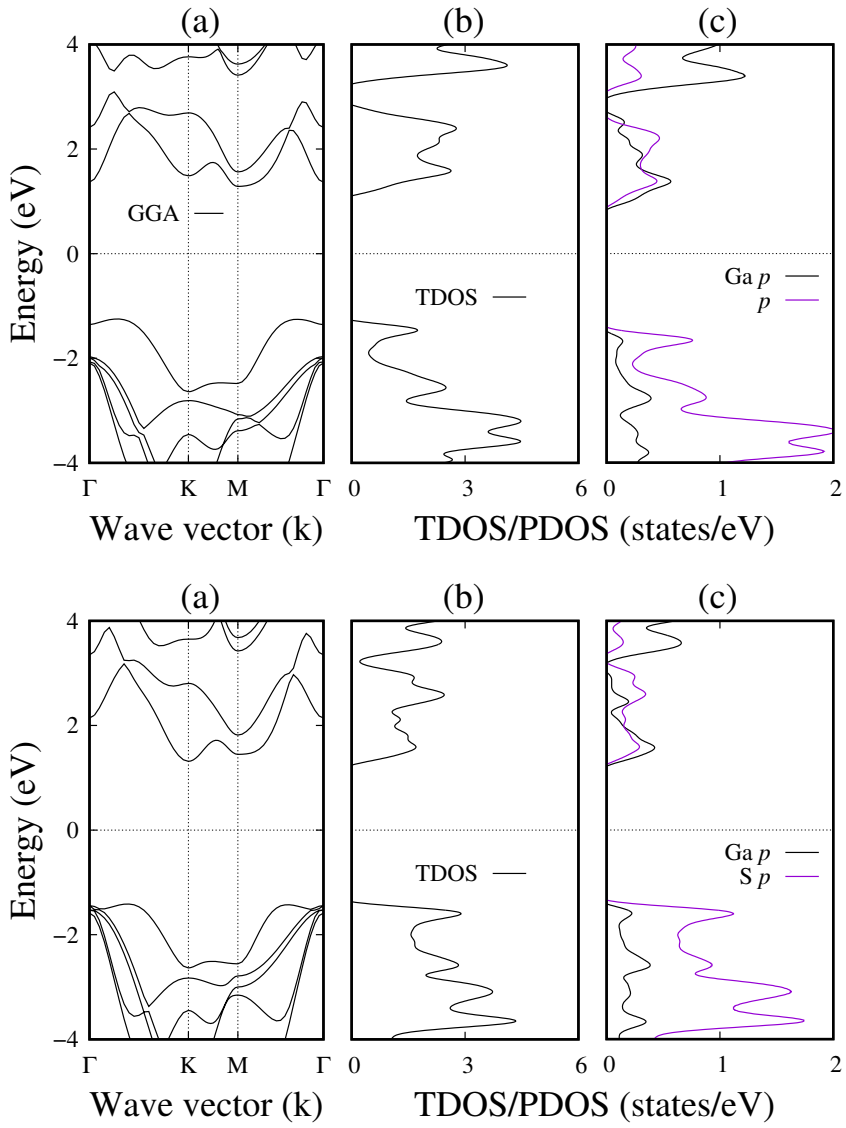

Figure SI 4: GGA+PBE calculated electronic band structure TDOS amd PDOS of GaS monolayer at equilibrium lattice constant (Top Figure) and average lattice constant (Bottom Figure), (a) electronic band structure (b)TDOS, and (c) PDOS of Ga p-orbital, and S atoms p-orbital are represented by black and purple color lines. The Fermi energy level is indicated by black dotted horizontal line.

$$R(\omega) = \frac{(1-n)^2 + k^2}{(1+n)^2 + k^2} \tag{8}$$

$$L(\omega) = \frac{\epsilon_2(\omega)}{\epsilon_1^2(\omega) + \epsilon_2^2(\omega)} \tag{9}$$

Here $L(\omega)$ is electron energy loss function [16] which is derived from the $\epsilon_1(\omega)$ and $\epsilon_2(\omega)$. An

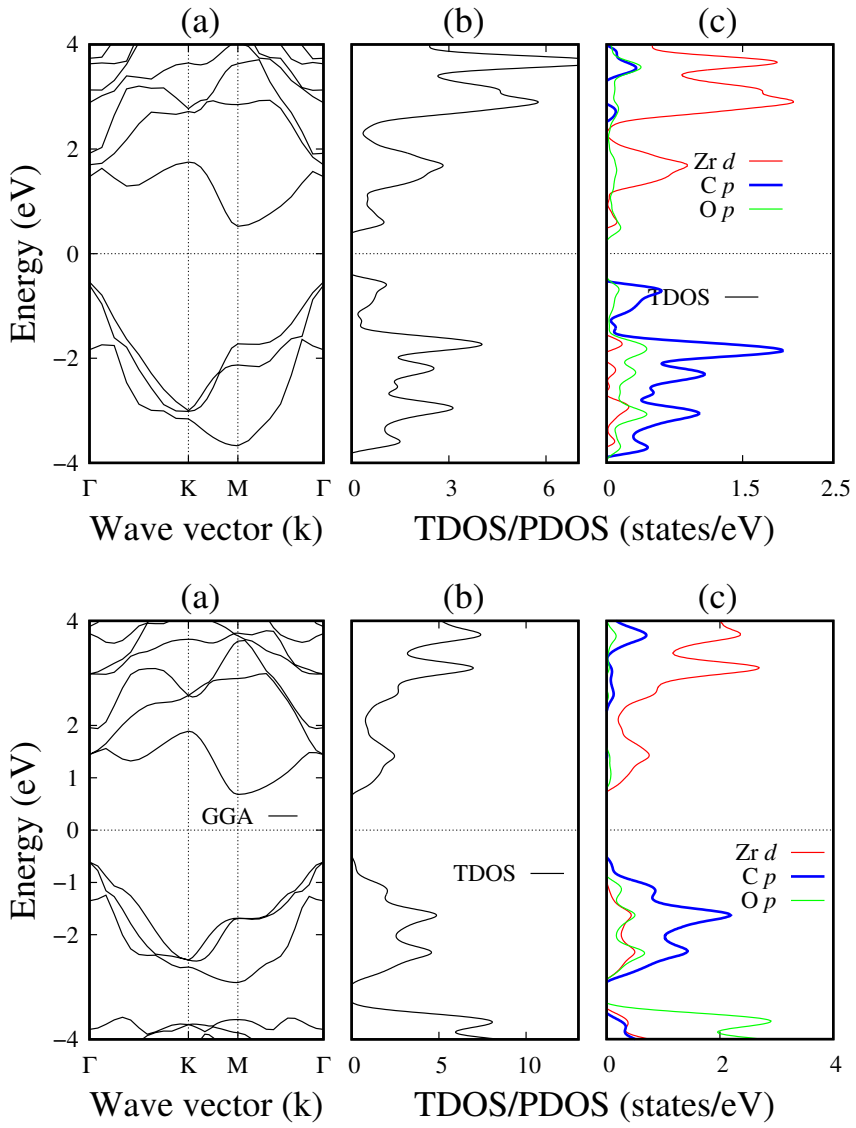

Figure SI 5: GGA+PBE calculated electronic band structure TDOS amd PDOS of Zr_2CO_2 monolayer (MD4 configuration) at equilibrium lattice constant a = 3.25 Å (Top) and at lattice constant a = 3.42 Å (Bottom), (a) electronic band structure (b)TDOS, and (c) PDOS of Zr *d*-orbital, C and O atoms *p*-orbital are represented by red, blue and green color lines. The Fermi energy level is indicated by black dotted horizontal line.

electron energy loss function is an essential idea in materials science and condensed matter physics is the electron energy loss function (EELF). It accounts for the energy that is lost by an incident electron as it travels through a substance as a result of interactions with the electrons in the substance. This phenomenon is frequently seen via experimental methods like electron energy loss spectroscopy (EELS) [16], and it has applications in a number of disciplines, such as solid-state

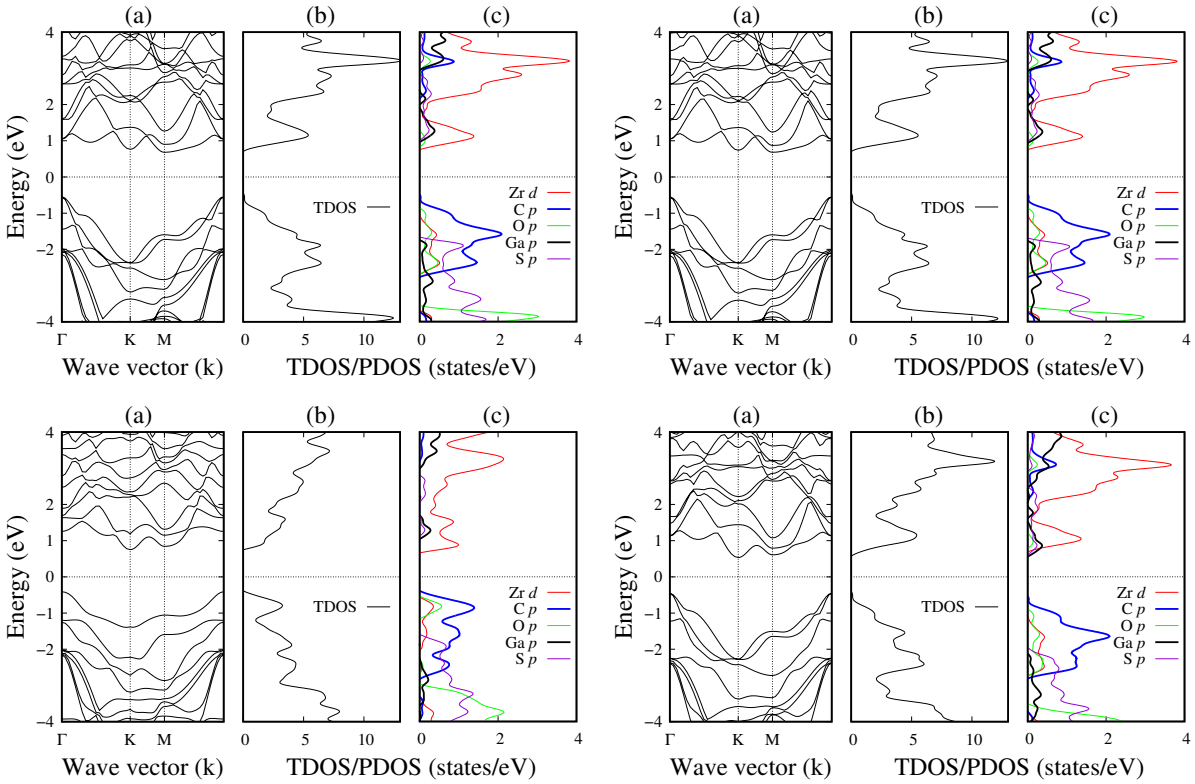

Figure SI 6: GGA+PBE calculated electronic band structure TDOS amd PDOS of all possible configuration of Zr_2CO_2/GaS van der Waals heterostructures ($\phi = 0^o$)„ (a) electronic band structure (b)TDOS, and (c) PDOS of Zr d-orbital, C and O atoms p-orbital are represented by red, blue and green color lines. The Fermi energy level is indicated by black dotted horizontal line.

physics, surface science, and nanotechnology.

REFERENCES

[1] W. Kohn, L. J. Sham, Self-consistent equations including exchange and correlation effects, Physical review 140 (4A) (1965) A1133.

[2] P. Giannozzi, S. Baroni, N. Bonini, M. Calandra, R. Car, C. Cavazzoni, D. Ceresoli, G. L. Chiarotti, M. Cococcioni, I. Dabo, et al., QUANTUM ESPRESSO: a modular and open-source software project for quantum simulations of materials, Journal of physics: Condensed matter 21 (39) (2009) 395502.

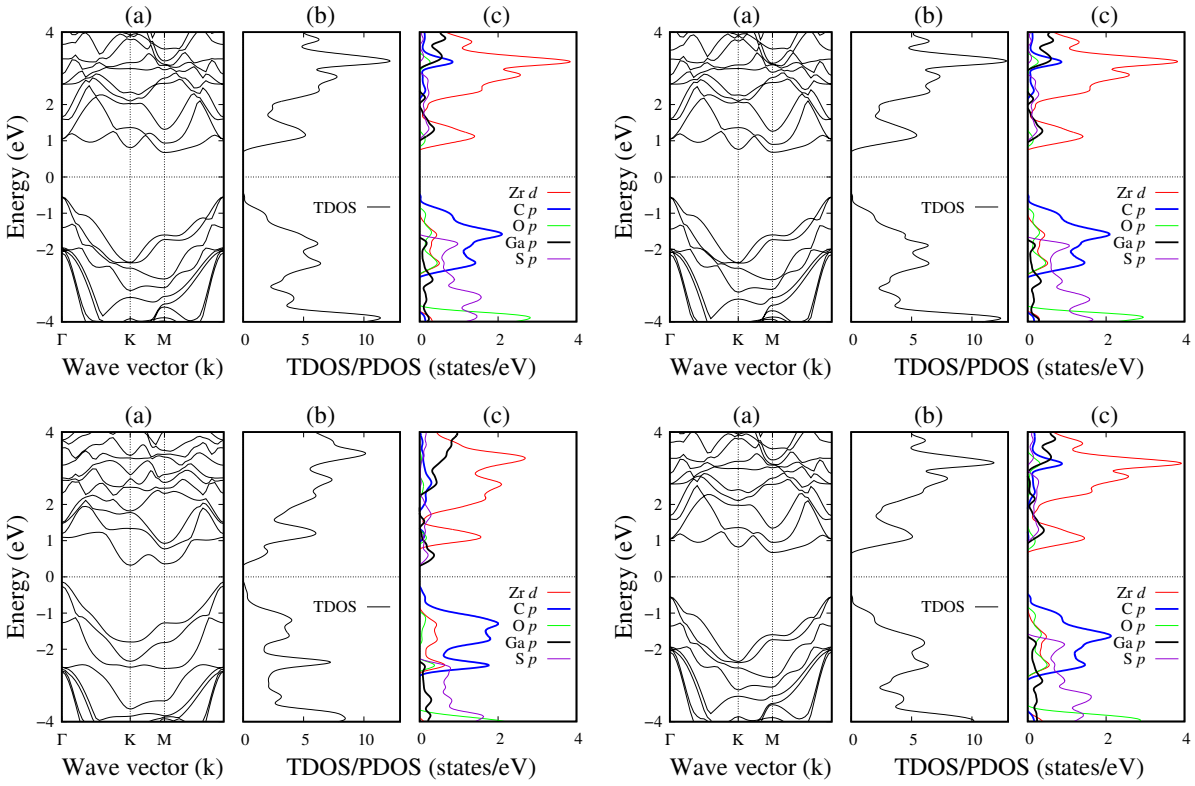

Figure SI 7: GGA+PBE calculated electronic band structure TDOS amd PDOS of all possible configuration of Zr_2CO_2/GaS van der Waals heterostructures ($\phi = 180^o$), (a) electronic band structure (b)TDOS, and (c) PDOS of Zr d-orbital, C and O atoms p-orbital are represented by red, blue and green color lines. The Fermi energy level is indicated by black dotted horizontal line.

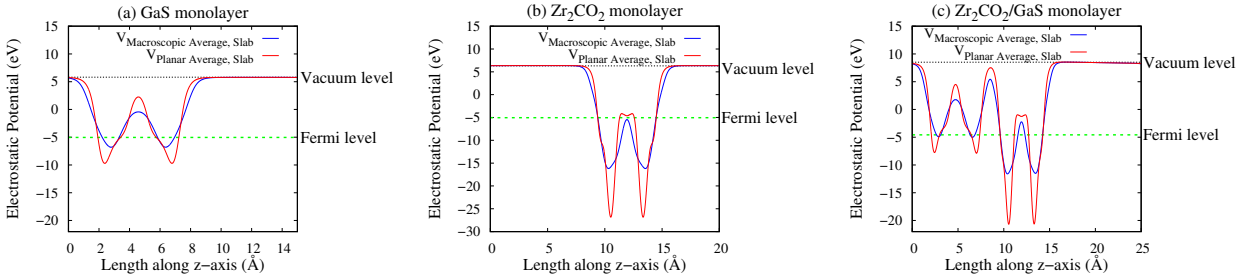

Figure SI 8: The calculated electrostatic potential of (a) an isolated GaS monolayer, (b) an isolated Zr_2CO_2 monolayer, and (c) MD4/GaS ($\phi = 0^o$) vdW heterostructures is calculated using the HSE energy functional. The Fermi energy level and vacuum energy level labels on the y2-axis are represented by green and black dotted horizontal lines, respectively.

[3] J. P. Perdew, K. Burke, M. Ernzerhof, Generalized gradient approximation made simple, Physical review letters 77 (18) (1996) 3865.

[4] H. J. Monkhorst, J. D. Pack, Special points for Brillouin-zone integrations, Physical review B 13 (12) (1976) 5188.

[5] A. U. Rahman, J. M. Morbec, G. Rahman, P. Kratzer, Commensurate versus incommensurate heterostructures of group-iii monochalcogenides, Physical Review Materials 2 (9) (2018) 094002.

[6] J. Heyd, G. E. Scuseria, M. Ernzerhof, Hybrid functionals based on a screened coulomb potential, The Journal of chemical physics 118 (18) (2003) 8207–8215.

[7] T. Kaewmaraya, M. Ramzan, H. Löfås, R. Ahuja, Hybrid density functional study of electronic and optical properties of phase change memory material: Ge 2 sb 2 te 5, Journal of Applied Physics 113 (3) (2013) 033510.

[8] M. Khan, A. Kashyap, A. Solanki, T. Nautiyal, S. Auluck, Interband optical properties of Ni_3Al, Physical Review B 48 (23) (1993) 16974.

[9] F. Wooten, Optical properties of solids, American Journal of Physics 41 (7) (1973) 939–940.

[10] N. V. Smith, Photoelectron energy spectra and the band structures of the noble metals, Physical Review B 3 (6) (1971) 1862.

[11] C. Ambrosch-Draxl, J. O. Sofo, Linear optical properties of solids within the full-potential linearized augmented planewave method, Computer physics communications 175 (1) (2006) 1–14.

[12] M. Fox, Optical properties of solids: Oxford university press (2001).

[13] F. Kong, G. Jiang, Nonlinear optical response of wurtzite ZnO from first principles, Physica B: Condensed Matter 404 (16) (2009) 2340–2344.

[14] S. Singh, Refractive index measurement and its applications, Physica Scripta 65 (2) (2002) 167.

[15] S. Kasap, Springer handbook of electronic and photonic materials, Springer Science & Business Media, 2006.

[16] P. Rani, G. S. Dubey, V. Jindal, DFT study of optical properties of pure and doped graphene, Physica E: Low-dimensional Systems and Nanostructures 62 (2014) 28–35.